Published online 1 June 2016

Nucleic Acids Research, 2016, Vol. 44, No. 17 ***8153–8164***
doi: 10.1093/nar/gkw498

FOXA1 potentiates lineage-specific enhancer activation through modulating TET1 expression and function

Yeqing A. Yang[1,†], Jonathan C. Zhao[1,†], Ka-wing Fong[1], Jung Kim[1], Shangze Li[1], Chunxiao Song[2], Bing Song[1], Bin Zheng[1], Chuan He[2,3] and Jindan Yu[1,4,*]

[1]Division of Hematology/Oncology, Department of Medicine, Northwestern University Feinberg School of Medicine, Chicago, IL 60611, USA, [2]Department of Chemistry, Department of Biochemistry and Molecular Biology, and Institute for Biophysical Dynamics, the University of Chicago, Chicago, IL 60637, USA, [3]Howard Hughes Medical Institute, the University of Chicago, Chicago, IL 60637, USA and [4]Robert H. Lurie Comprehensive Cancer Center, Northwestern University Feinberg School of Medicine, Chicago, IL 60611, USA

Received September 29, 2015; Revised May 23, 2016; Accepted May 24, 2016

ABSTRACT

Forkhead box A1 (FOXA1) is an FKHD family protein that plays pioneering roles in lineage-specific enhancer activation and gene transcription. Through genome-wide location analyses, here we show that FOXA1 expression and occupancy are, in turn, required for the maintenance of these epigenetic signatures, namely DNA hypomethylation and histone 3 lysine 4 methylation. Mechanistically, this involves TET1, a 5-methylcytosine dioxygenase. We found that FOXA1 induces TET1 expression via direct binding to its cis-regulatory elements. Further, FOXA1 physically interacts with the TET1 protein through its CXXC domain. TET1 thus co-occupies FOXA1-dependent enhancers and mediates local DNA demethylation and concomitant histone 3 lysine 4 methylation, further potentiating FOXA1 recruitment. Consequently, FOXA1 binding events are markedly reduced following TET1 depletion. Together, our results suggest that FOXA1 is not only able to recognize but also remodel the epigenetic signatures at lineage-specific enhancers, which is mediated, at least in part, by a feed-forward regulatory loop between FOXA1 and TET1.

INTRODUCTION

Forkhead box A1 (FOXA1; also known as hepatocyte nuclear factor 3 α or HNF3A) belongs to the forkhead family of transcription factors and is known to play a pivotal role for the postnatal development of the mammary and prostate glands (1). FOXA1 is critical in directing hormone receptor-dependent transcriptional programs to regulate prostate- or breast-specific gene expression and cell differentiation (2,3). FOXA1 acts as a 'pioneer transcription factor' that can associate with compact chromatin to increase local chromatin accessibility and facilitate the recruitment of other transcription factors including nuclear receptors to these sites (4). Genome-wide location analyses have reported that FOXA1 preferentially recognizes and binds lineage-specific enhancers that are demarcated by active histone modifications including histone H3 lysine 4 mono- and di-methylation (H3K4me1, me2) (5), histone 27 acetylation (H3K27ac) (6), as well as local DNA hypomethylation (7). On the other hand, enforced expression of FOXA1 and its subsequent recruitment to enhancers lead to DNA demethylation and *de novo* gain of H3K4me1, suggesting that FOXA1 is able to remodel heterochromatic regions (7,8). However, the molecular mechanisms by which FOXA1 imposes this chromatin remodeling have not been characterized.

TET (ten-eleven translocation) proteins are a family of DNA hydroxylases that oxidize the methyl group at the C5 position of methylated cytosine, enzymatically converting 5-methylcytosine (5mC) into 5-hydroxymethylcytosine (5hmC), 5-formylcytosine (5fC) and 5-carboxylcytosine (5caC) in a sequential and iterative manner, ultimately leading to the removal of DNA methylation (9,10). Through catalyzing DNA demethylation, TET proteins play important roles in embryonic stem cell maintenance and in regulating appropriate lineage differentiation of these cells. These activities can be linked to the ability of DNA demethylation in modulating transcription factor occupancy and *vice versa* (11,12). During neural and adipocyte differentiation, dynamic hydroxmethylation has been associated with lineage-specific distal regulatory regions and represents an early

*To whom correspondence should be addressed. Tel: +1 312 503 1761; Fax: +1 312 503 0189; Email: jindan-yu@northwestern.edu
†These authors contributed equally to the paper as first authors.

event of enhancer activation (13). Concordantly, a separate study has demonstrated that deletion of Tet2 led to extensive loss of 5hmC and gain of DNA hypermethylation at enhancers and modulates enhancer activity of differentiation-related genes (14). However, the roles of TET proteins in FOXA1 recruitment and regulation of prostate lineage-specific enhancers are yet to be delineated.

Here, we show that TET1 is a direct target of FOXA1-mediated transcriptional activation. Further, TET1 physically interacts with the FOXA1 protein and modulates local DNA demethylation that in turn facilitates and stabilizes the recruitment of FOXA1. FOXA1 and TET1 thus form a feed-forward loop that activates lineage-specific enhancers. Not only does this mechanism provide a new perspective on the dynamic functional significance of the newly discovered TET1 DNA hydroxylase, but also offer insight into the molecular details underlying FOXA1's ability to fine-tune and modulate lineage-specific enhancer activation. As FOXA1 is a critical regulator and a top mutated gene in multiple cancers such as breast and prostate cancers (15), our study thus forms the framework for future understanding of the roles of TET1 in lineage-specific gene expression and cancer progression.

MATERIALS AND METHODS

Cell lines, plasmids and antibodies

Prostate cancer cell lines LNCaP, VCaP, 22Rv1, BPH1, RWPE-1, DU145 and human embryonic kidney cell line HEK293T cells were obtained from American Type Culture Collection and cultured in either RPMI1640 or Dulbecco's modified Eagle's medium with 10% fetal bovine serum (FBS). For FOXA1 and TET1 FL and domain constructs, human FOXA1 and TET1 cDNA were amplified by reverse transcription polymerase chain reaction (PCR) from LNCaP cells and pENTR223 TET1 (Harvard Plasmid), respectively, and cloned into the entry vector pCR8/GW/TOPO (Invitrogen). Adenoviral construct expressing FOXA1 was generated by recombining pCR8-FOXA1 with pAD/CMV/V5 using LR Clonase II (Invitrogen). Overexpression constructs for TET1 were generated by recombination of pCR8-TET1 with NTSFB destination vector or pLenti CMV/TO Puro DEST (Addgene plasmid 17 293). The pGIPZ lentiviral control and FOXA1 shRNAs were purchased from Open Biosystems. Sequences for scramble (5′-GCGCGCTTTGTAGGATTCG-3′) and TET1 (5′-GTGGAGAAGTGGACACAAA-3′) shRNA were kindly provided by Dr Debabrata Chakravarti (Northwestern University), and cloned into pLKO lentiviral vector.

The antibodies used in this study include anti-FOXA1 (ab23738) and anti-GAPDH (ab9385) from Abcam, anti-TET1 (GTX627420 and GTX124207) from GeneTex, anti-FLAG (F1804 and F7425) from Sigma, anti-c-Myc (sc-789x) from Santa Cruz, anti-HA (ab9110) from Abcam, anti-alpha Tubulin (sc-32293) from Santa Cruz, anti-5mC (BI-MECY-0100) from Eurogentec, anti-5hmC (39769) from Active Motif, anti-H3K4me2 (07-030) from Millipore, anti-H3K27ac (ab4279) from Abcam.

Luciferase reporter assay

TET1 promoter and enhancer luciferase reporter assays were conducted according to the manual of Dual-Luciferase Reporter Assay System from Promega. Briefly, LNCaP cells were seeded in a 24-well plate and co-transfected with the Renilla expression plasmid pRL-TK and the reporter constructs for TET1 promoter and enhancer in pGL4 vector. Cells were infected with LacZ (control) or FOXA1 adenovirus for 48 h to assess the effect of FOXA1 overexpression on luciferase activity. Conversely, to look at FOXA1 depletion effect, lentiviral-transduced shCtrl and shFOXA1 LNCaP cells were used for co-transfection of reporter constructs. Luciferase activities were determined 48–72 h post-transfection and normalized against Renilla internal control values.

Immunofluorescence staining

Cells were fixed with 4% formaldehyde for 15 min at RT and then permeabilized in 0.1% Triton X-100 for 15 min at RT. Cells were then washed by phosphate buffered saline (PBS) for three times, followed by incubation with 5% normal goat serum for 30 min at RT. Subsequently, cells were incubated with primary antibody, the anti-FLAG antibody (Sigma) and anti-TET1 (Genetex), for 2 h at RT. After washing three times with PBS, cells were incubated with secondary antibody, Alexa Fluor 488 and 594 goat anti-rabbit IgG (Invitrogen), for 1h at RT. Finally, cells were washed three times with PBS and mounted using Prolong Gold Antifade Reagent (Invitrogen).

Co-immunoprecipitation

Nuclear proteins were extracted from 293T or LNCaP cells (details provided in Supplementary Methods). For S protein pulldown, nuclear extracts were incubated with 30 μl S-protein agarose beads (Millipore) for 3 h at 4°C. The beads/protein complex was then washed four times, and eluted with 30 μl 2× sodium dodecyl sulphate (SDS) sample buffer and subjected to western blot analysis. For LNCaP endogenous co-immunoprecipitation (co-IP), nuclear extracts were incubated with 2 μg antibodies, anti-FOXA1 (Abcam), anti-TET1 (Genetex) and anti-rabbit IgG (Santa Cruz) overnight at 4°C. Dynabeads Protein A (Life Technologies), 25 μl per immunoprecipitation (IP), were added the next day and incubated for 1 h at 4°C. Similarly, the beads/protein complex was washed four times, and eluted with 30 μl 2× SDS sample buffer and subjected to western blot analysis.

Chromatin immunoprecipitation (ChIP)

Chromatin immunoprecipitation (ChIP) experiments were carried out as previously described (16). All primers (listed in Supplementary Data) were designed using Primer 3 (http://frodo.wi.mit.edu/primer3/), synthesized by Integrated DNA Technologies and used for SYBR Green based real-time PCR. ChIP-quantitative PCR enrichment of target loci was normalized to input DNA and reported as Enrichment over input ±SEM. ChIP DNA was prepared into

libraries according to standard protocols using Bioo Scientific's DNA Sample Kit (cat. no. 514101). Libraries were sequenced using Illumina Hi-Seq platforms. Sequence reads were aligned to the Human Reference Genome (assembly hg19) using Burrows–Wheeler alignment tool (bwa) version 0.6.1. New high-throughput data generated in this study have been deposited in GEO database under accession number GSE73363.

Methylated DNA immunoprecipitation (MeDIP)

Methylated DNA immunoprecipitation (MeDIP) was performed as previously described (17). Total genomic DNA was extracted using QIAamp DNA Mini Kit (Qiagen) and sonicated to obtain fragments between 300 and 1000 bp. Dynabeads M-280 Sheep anti-Mouse IgG (Invitrogen) were incubated with an anti-5-methylcytidine antibody (BI-MECY_0100, Eurogentec, Fremont, CA, USA) overnight at 4°C. The following day, 4 μg of sheared DNA was denatured by boiling at 95°C for 10 min followed by rapid cooling on ice, and subsequently added to the beads/antibody complex. On day 3, the beads were washed three times with PBS + 0.05% Triton X-100 and eluted from beads by incubation at 65°C for 5 min in 150 μl elution buffer (TE + 1% SDS). Elution was repeated for a total of two times. Total eluates were treated with proteinase K and incubated at 50°C for 2 h. QIAquick PCR purification kit (Qiagen) was used to purify the eluted DNA, and lastly qPCR was used to determine the enrichment of target genomic regions using gene-specific primers (listed in Supplementary Data). Enrichment of target loci was normalized to input DNA and reported as Enrichment over input ±SEM.

5hmC chemical labeling (hMe-Seal)

5hmC labeling experiments were performed as previously described (18). Briefly, genomic DNA was fragmented to an average of 400 bp and was incubated with 50 mM HEPES buffer (pH 7.9), 25 mM MgCl2, 100 mM UDP-6-N3-Glc and 2 mM βGT for 1 h at 37°C. The labeled DNA was purified by the QIAquick Nucleotide Removal kit (Qiagen) and eluted in H_2O. The click chemistry was performed with the addition of 150 mM of disulfide-biotin, and the mixture was incubated for 2 h at 37°C. The labeled DNA fragments were then purified by the QIAquick Nucleotide Removal kit (Qiagen) and enriched by Dynabeads Streptavidin C1 (Invitrogen), and subsequently released by dithiothreitol (DTT) treatment. The enriched DNA fragments were first purified by Micro Bio-Spin 6 spin columns (Bio-Rad) followed by MinElute PCR Purification Kit (Qiagen).

RESULTS

FOXA1 expression contributes to lineage-specific enhancer activation

To determine the correlation between FOXA1 and active enhancer marks, we re-analyzed previously published FOXA1 (GSE37345), H3K4me2 and H3K27ac ChIP-seq data (GSE27823) (19,20) and confirmed that FOXA1 binding sites (FXBS) are indeed enriched for H3K4me2 and H3K27ac (Figure 1A: top). Further, we performed MeDIP for 5mC and chemical labeling of 5hmC followed by deep sequencing, namely MeDIP-seq and hMe-Seal-seq (18,21), respectively, to map their genomic landscapes in LNCaP cells which express FOXA1. Bioinformatic analysis revealed that FXBS are depleted of 5mC, but enriched for 5hmC, being consistent with previous reports (7). In addition, we found that this correlation was much weaker in two other prostate cell lines namely PrEC and PC-3M, wherein FOXA1 expression is low, suggesting that FOXA1 expression and occupancy might contribute to DNA demethylation at local chromatin (Supplementary Figure S1A–C). Since it has been previously suggested that transcription factor binding sites can demonstrate the low 5mC high 5hmC signature in embryonic stem cells (12), we looked at DNA methylation profiles in LNCaP cells for two other transcription factors CTCF and AR and observed similar patterns for 5mC and 5hmC (Supplementary Figure S2A–D). As a measure of negative control, genomic regions 20 kb downstream from the FOXA1 peaks, which will be referred to as non-peak sites throughout this paper, were examined for epigenetic signatures but did not exhibit any distinct pattern (Figure 1B: bottom).

To further elaborate on this, we depleted FOXA1 in LNCaP cells through lentiviral shRNA transduction (Supplementary Figure S1D) and performed pulldown and deep sequencing of 5mC and 5hmC. Interestingly, although the average intensity of 5mC around all FOXA1-occupied sites was not hugely affected upon FOXA1 depletion (Figure 1B), there was a significant decrease in 5hmC (Figure 1C), whereas no changes were seen in either 5mC or 5hmC for non-peak sites (Figure 1D and E). Concordantly, active enhancer marks H3K4me2 and H3K27ac were decreased around FXBS following FOXA1 knockdown, supporting reduced enhancer activities (Supplementary Figure S1E and F). To ensure the reliability of this genome-wide phenomenon, as well as to examine the changes with a more sensitive method, we performed MeDIP and hMe-Seal followed by qPCR for individual genes. Expectedly, 5hmC was greatly reduced across a number of FXBS (Figure 1F). On the other hand, despite the fact that 5mC showed no obvious change on a global scale, MeDIP-PCR revealed moderate increases in 5mC upon FOXA1 knockdown (Supplementary Figure S3). Taking into consideration that 5hmC abundance represents only ∼10% of 5mC in embryonic stem cells (9), it is reasonable to observe a more significant change in 5hmC rather than 5mC. It can be inferred from these results that FOXA1 may be functioning to alter DNA methylation specifically at regions where it occupies to achieve a demethylated state while accumulating 5hmC marks, thus potentiating enhancer activation.

FOXA1 positively regulates TET1 gene expression.

As DNA demethylation has recently been shown catalyzed by the TET proteins, we next examined whether TET gene expression is associated with FOXA1. We first performed qRT-PCR analysis of FOXA1 and TET1 transcript across a panel of 12 prostate cell lines (Figure 2A and B). Interestingly, like FOXA1, TET1 is in general expressed at a much higher level in AR-positive prostate cancer cell lines such as C4-2B and VCaP cells than in AR-negative cells includ-

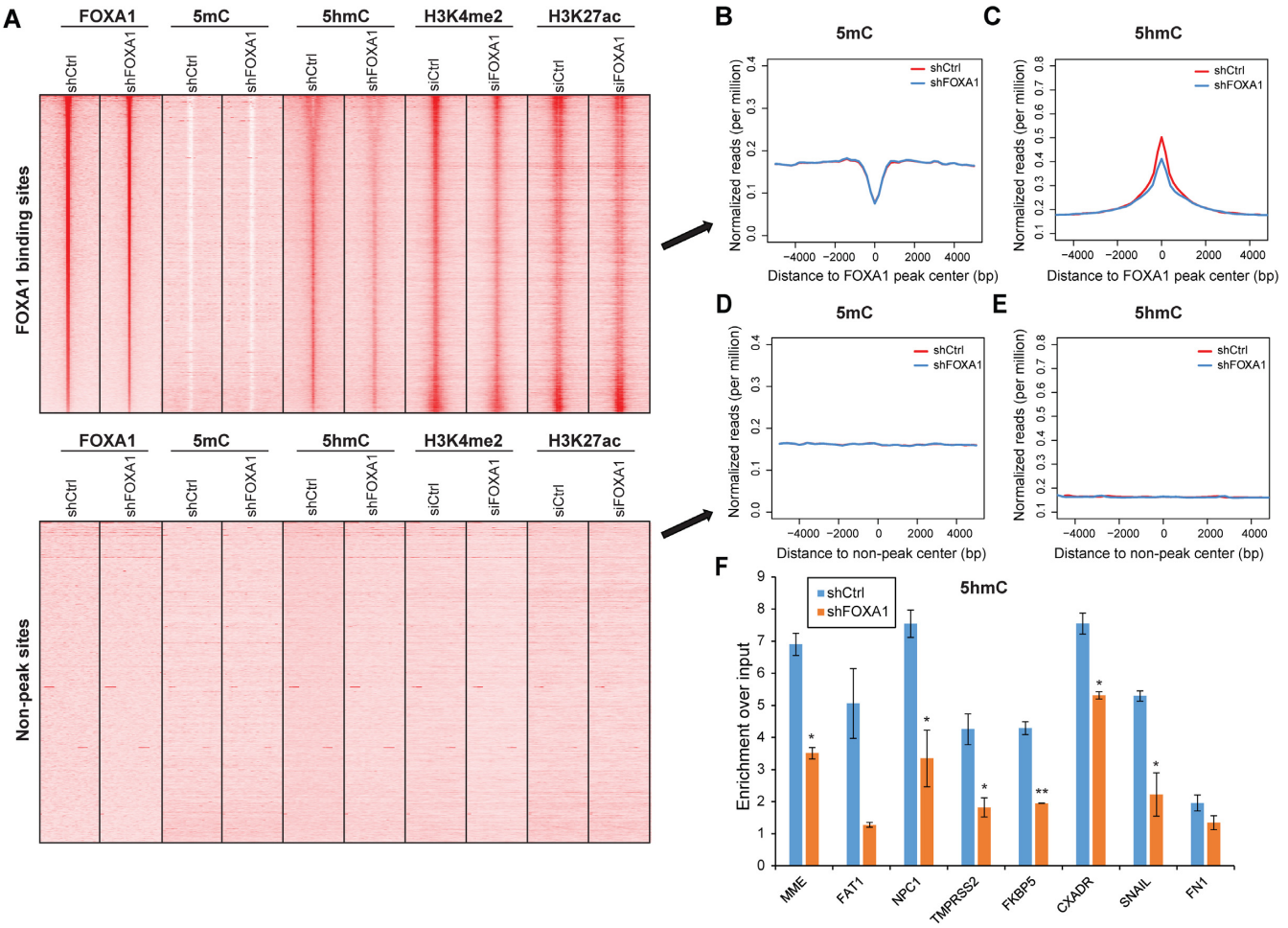

Figure 1. FOXA1 contributes to enhancer activation through epigenetic modifications. (**A**) Epigenetic signatures of FOXA1 binding sites (FXBS) (top panel) and non-peak sites taken 20 kb downstream (bottom panel) in control and shFOXA1 LNCaP cells. FOXA1 and H3K4me2/H3K27ac ChIP-seq data were obtained from publicly available datasets GSE37345 and GSE27823, respectively. Genomic landscapes of 5mC and 5hmC were determined by MeDIP and hMe-Seal, respectively, followed by deep sequencing. ChIP-seq read intensities of indicated epigenetic marks around (±5 kb) FXBS or non-peak regions in control (shCtrl) and FOXA1-knockdown (shFOXA1) cells were presented in heatmap format, ranked by read intensity of FOXA1 occupancy. (**B** and **C**) Average intensity plots of 5mC (B) and 5hmC (C) enrichment around all FXBS shown in A: top. (**D** and **E**) Average intensity plots of 5mC (D) and 5hmC (E) enrichment around all non-peak sites shown in A: bottom. (**F**) Locus-specific change in 5hmC by qPCR of hMe-Seal at representative FXBS for control and shFOXA1 LNCaP cells. Data shown is mean ± SEM of technical replicates from one representative experiment out of two. $*P < 0.05$ and $**P < 0.01$.

ing DU145 and RWPE. Further analysis showed that TET1 expression level is highly correlated ($r = 0.96$, $P < 0.001$) with that of FOXA1 (Supplementary Figure S4). This positively correlated expression between FOXA1 and TET1 was confirmed in three large prostate cancer patient datasets (Supplementary Figure S5A–C). As the correlation between FOXA1 and other TET proteins is relatively weaker, we decided to focus on TET1 in this study.

Since TET1 exhibited a similar expression pattern to FOXA1, we asked whether FOXA1 regulates TET1 gene expression. To test this, we first examined TET1 level in LNCaP cells with control or FOXA1 knockdown. Importantly, both TET1 transcript and protein levels were markedly decreased in LNCaP cells following FOXA1 knockdown (Figure 2C and D; Supplementary Figure S5D). Concordantly, depletion of FOXA1 in another independent prostate cancer cell lines C4-2B also resulted in a decrease in TET1 expression (Figure 2E). On the other hand, when FOXA1 was overexpressed in 22Rv1 cells through adenovirus infection, TET1 expression was augmented (Figure 2F), which was further validated in another prostate cancer cell line DU145 that contained low endogenous FOXA1 level (Figure 2G). To visualize the inductive effect of FOXA1 on TET1 at the cellular level, we performed immunofluorescence staining. TET1 was barely detectable in control DU145 cells infected with empty vector adenovirus (Figure 2H, top panel). However, upon infection with adenoviral FOXA1 (Flag-tagged, shown in red), TET1 staining (shown in green) was significantly enhanced (middle panel). Specifically, TET1 was stained positively in the majority of cells that had FOXA1 infection and overexpression, but not in the uninfected cells, as further illustrated in the zoomed-in microscopy images (Figure 2H, bottom panel). Taken together, our data support that FOXA1 positively regulates TET1 gene transcription.

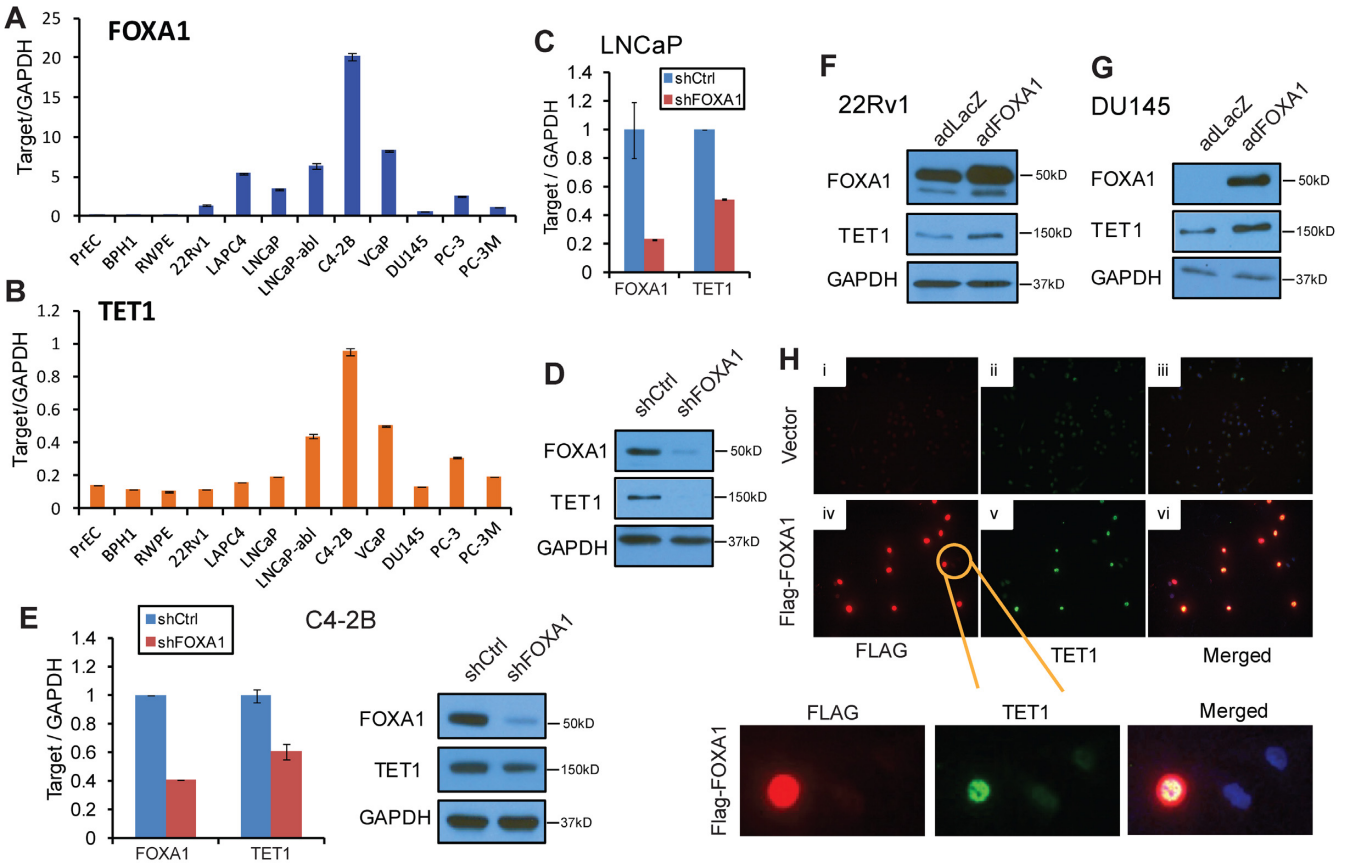

Figure 2. FOXA1 induces TET1 gene expression. (**A** and **B**) Correlated FOXA1 and TET1 gene expression in prostate cells. RNA was extracted from a panel of 12 prostate cell lines and analyzed by qRT-PCR for FOXA1 (A) and TET1 (B) gene expression. Data shown are mean ± SEM of technical replicates from one representative experiment out of three. (**C** and **D**) TET1 transcript (C) and protein (D) are downregulated following FOXA1 knockdown in LNCaP cells. LNCaP cells were infected with shCtrl or shFOXA1 lentivirus and subsequently subjected to qRT-PCR and western blot analysis. Data shown are one representative out of triplicate experiments. (**E**) TET1 is downregulated by FOXA1 knockdown in C4-2B cells. C4-2B cells were infected with shCtrl or shFOXA1 lentivirus for 8 h followed by puromycin selection for 4 days, and subsequently subjected to qRT-PCR and western blot analysis. Data shown are one representative out of triplicate experiments. (**F** and **G**) TET1 is upregulated following FOXA1 overexpression. The 22Rv1 (F) and DU145 (G) cells were infected with LacZ or FOXA1 adenovirus for 48 h and immunoblot was performed to assess FOXA1 and TET1 protein levels. (**H**) Positive TET1 staining in FOXA1-expressing cells. DU145 cells were infected with LacZ control (i–iii) or Flag-tagged FOXA1 (iv–vi) adenovirus for 48 h and then subjected to Immunofluorescence co-staining of FOXA1 and TET1. Bottom panel shows zoomed-in region containing both FOXA1-uninfected and -infected cells.

TET1 is a direct transcriptional target of FOXA1

To determine how FOXA1 transcriptionally controls TET1 expression, we examined FOXA1 ChIP-seq data previously obtained from LNCaP cells (20), and observed a strong FOXA1 binding event within the intragenic region, between exons 3 and 4, of the TET1 gene (Figure 3A). Being consistent with FOXA1 as an enhancer regulator that modulates target genes through enhancer–promoter looping, we also found a weak FOXA1 binding event at the TET1 promoter. To validate the results of ChIP-seq, we performed ChIP-qPCR in LNCaP cells and found that FOXA1 is enriched at the TET1 enhancer for nearly 170-fold relative to IgG control, an enrichment level comparable to that at the Prostate-Specific Antigen (PSA, or KLK3) gene enhancer, and for about 10-fold at the TET 1 promoter (Figure 3B). A similarly strong enrichment of FOXA1 at the TET1 enhancer and promoter was also observed in an additional FOXA1-expressing cell line C4-2B (Supplementary Figure S6). Moreover, upon lentiviral knockdown, FOXA1 binding to its target site for the PSA gene was greatly diminished as expected, and similarly for TET1 enhancer and promoter, confirming that the ChIP enrichment signal was specific for FOXA1 (Figure 3C). Next, to examine whether FOXA1 occupancy at the TET1 enhancer and promoter leads to regulation of their transcriptional activities, we cloned these regions into reporter constructs. Luciferase assays showed that FOXA1 overexpression indeed significantly increased, whereas FOXA1 knockdown decreased, TET1 enhancer and promoter activities (Figure 3D and E). To further demonstrate that this regulation is due to FOXA1 occupancy at the TET1 enhancer and promoter, we analyzed the DNA sequences around the FOXA1 binding peaks for FKHD motifs within the TET1 enhancer as well as promoter. Through mutagenesis assays, we generated TET1 enhancer and promoter constructs with mutations to highly conserved FKHD motifs (Figure 3A, bottom panels). Importantly, luciferase assays revealed that mutations to the FKHD motifs abolished FOXA1 regulation of TET1

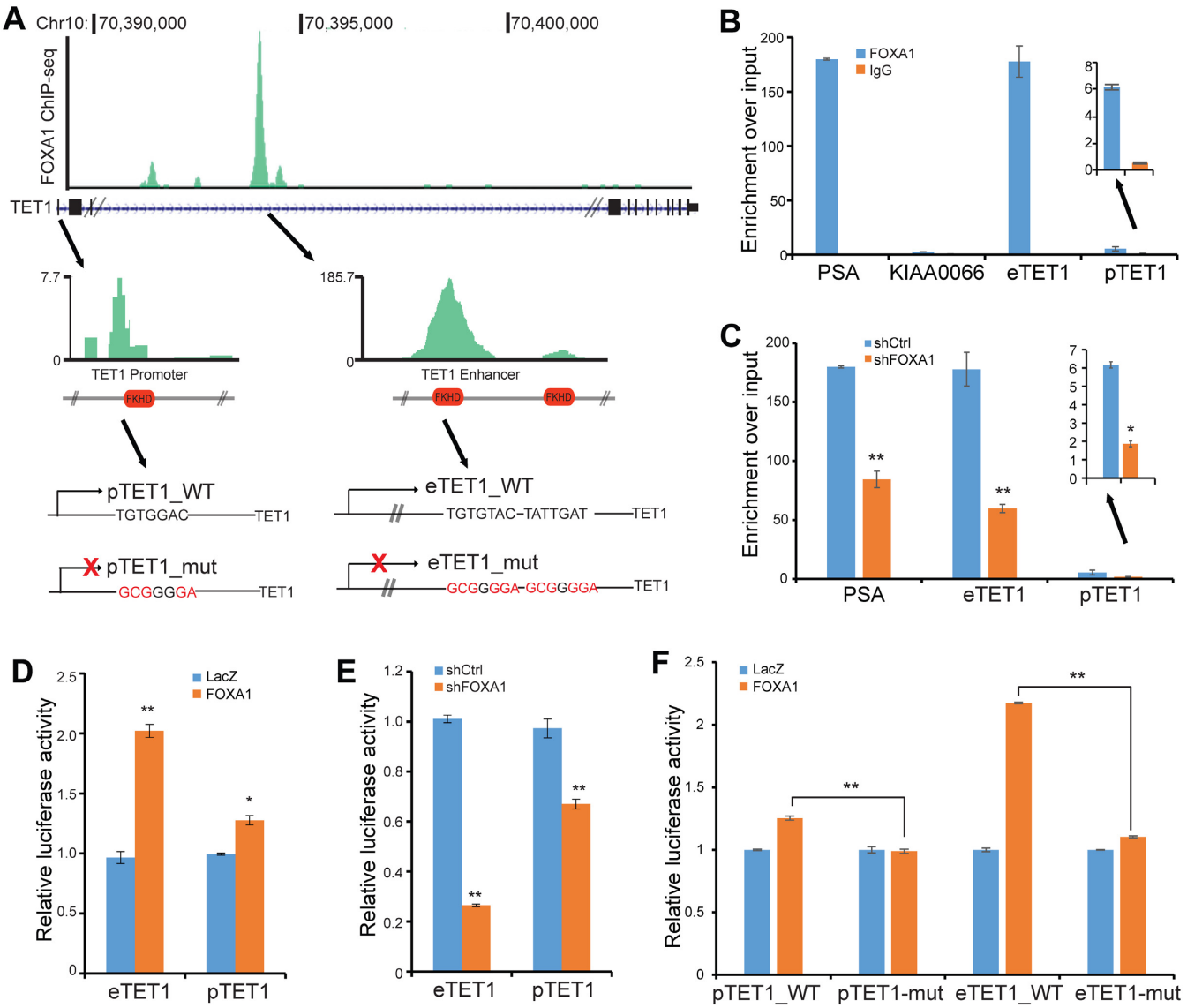

Figure 3. TET1 is a direct transcriptional target of FOXA1. (**A**) ChIP-seq showing FOXA1 binding events at TET1 promoter and enhancer. FOXA1 ChIP-seq was conducted in LNCaP cells and FOXA1 binding events were identified by HOMER and visualized in UCSC Genome Browser. FKHD motifs (indicated by red box) near FXBS were determined by JASPAR. DNA fragments containing FXBS at the TET1 promoter (pTET1) and enhancer (eTET1) were each cloned into pGL4 luciferase reporter construct with wild-type (WT) or mutated (mut) FKHD motif (mutated nt shown in red at the bottom panel). (**B**) ChIP-PCR validation of FOXA1 binding to TET1 enhancer and promoter in LNCaP cells. ChIP was performed using anti-FOXA1 and anti-IgG antibodies in LNCaP cells. ChIP-qPCR was performed using primers flanking the FOXA1 binding peaks at the TET1 enhancer (eTET1) and promoter (pTET). PSA is used as a positive control while KIAA0066 a negative control. Data shown are mean ± SEM of technical replicates from one representative experiment out of three. (**C**) FOXA1 occupancy at TET1 promoter and enhancer was decreased by FOXA1 knockdown. ChIP-qPCR using anti-FOXA1 antibody was carried out in control and FOXA1-depleted LNCaP cells. Data shown are mean ± SEM of technical replicates from one representative experiment out of three. $*P < 0.05$ and $**P < 0.01$. (**D** and **E**) FOXA1 positively regulates TET1 enhancer and promoter activities. TET1 enhancer and promoter reporter constructs were transfected into LNCaP cells with control or FOXA1 overexpression (D) and LNCaP cells with control or FOXA1 knockdown (E) for 48 h. Luciferase activities were determined and normalized to internal control Renilla reporter. Data shown are mean ± SEM of two independent experiments. $*P < 0.05$ and $**P < 0.01$. (**F**) FKHD motif is required for FOXA1-induced TET1 promoter and enhancer luciferase activities. Control and FOXA1-overexpressing LNCaP cells were transfected with either WT or mutated (depicted in A) TET1 promoter and enhancer reporter constructs. Luciferase activities were determined and normalized to internal control Renilla reporter. Data shown are mean ± SEM of two independent experiments. $*P < 0.05$ and $**P < 0.01$.

enhancer as well as promoter activities (Figure 3F). Taken together, our data support that FOXA1 directly binds to the regulatory elements of TET1 gene to induce its transcription. As FOXA1 contributes to local DNA demethylation (Figure 1) and TET1 is a known DNA demethylase, we hypothesized that TET1 may be attributable for DNA demethylation around the FXBS. To test this hypothesis, we started out by examining potential interactions between the FOXA1 and TET1 proteins.

FOXA1 and TET1 proteins physically interact

By use of overexpression systems in 293T cells, we conducted co-IP experiments to assess whether physical interaction is present between ectopic FOXA1 and TET1 proteins. The 293T cells were co-transfected with Flag-tagged TET1 along with FOXA1 or empty vector. Successful expression of the ectopic proteins was confirmed by western blot analysis of the input lysate. IP using an anti-FOXA1 antibody followed by immunoblotting confirmed successful pulldown of FOXA1 itself as well as the TET1 protein, the latter only in the cells expressing both TET1 and FOXA1 (Figure 4A). To demonstrate the interaction through reversal co-IP, we cloned TET1 into the SFB-tagged expression vector, which enabled pulldown of the TET1 protein using S-protein agarose beads and detection by anti-Flag antibodies (22). Either SFB-vector control or SFB-TET1 was co-transfected with FOXA1 into 293T cells and their expression was confirmed by western blot analysis of the input lysate. S-protein pulldown followed by western blotting using anti-Flag validated successful enrichment of SFB-tag only or SFB-TET1 (of different sizes) in the corresponding lysates, while immunoblotting using anti-FOXA1 revealed FOXA1 pulldown only in the SFB-TET1-expressing cells (Figure 4B), supporting physical interaction between ectopic FOXA1 and TET1 proteins.

Next, we attempted to confirm this interaction between endogenous FOXA1 and TET1 proteins. LNCaP cell nuclear lysate was subjected to IP using rabbit anti-TET1, anti-FOXA1 and IgG control followed by western blotting with mouse anti-TET1 or anti-FOXA1 antibodies. Our results demonstrated that TET1 and FOXA1 antibodies are able to pull down each other, supporting strong protein interactions (Figure 4C). To address the potential involvement of DNA in mediating this interaction, we performed co-IP in the presence or absence of ethidium bromide. Notably, our results demonstrated persistent interaction between FOXA1 and TET1 proteins in the presence of ethidium bromide, thus indicating that DNA was not required for their association (Supplementary Figure S7A). Moreover, this interaction between endogenous FOXA1 and TET1 proteins was also confirmed in C4-2B cells (Supplementary Figure S7B).

To further determine which domains of the TET1 protein are important for its interaction with FOXA1, we generated four Myc-tagged TET1 domain constructs, namely the N-terminal, CXXC, middle and CD domains, which were co-transfected with SFB-tagged FOXA1 into 293T cells. S-protein pulldown followed by western blot analysis showed that only the TET1 fragment containing the CXXC module was able to bind FOXA1 (Figure 4D). On the other hand, we attempted to map out the FOXA1 domain that is responsible for its interaction with the TET1 protein. Similarly, we created three Flag-tagged FOXA1 domain constructs, namely N-terminal, Forkhead (FH) and C-terminal domains, which were co-transfected with SFB-tagged TET1-CXXC domain into 293T cells. Western blot analysis confirmed the expression of various FOXA1 domains of different sizes as expected (Figure 4E). S-protein pulldown of TET1 followed by western blotting revealed that only the FH-containing domain of FOXA1 protein is able to interact with the TET1-CXXC domain. Moreover, we also performed *in vitro* pulldown assay utilizing purified TET1-CXXC and FOXA1-FH domain proteins, which confirmed that the two proteins directly interact (Figure 4F). As the CXXC zinc finger module in Tet3 protein has been shown critical for specific chromatin targeting, while its enzymatic domain modulates its biological function (23), we hypothesized that TET1 interaction with FOXA1 through its CXXC domain may be important for its recruitment to FXBS where it carries out hydroxylation on methylated CpG's closeby through its CD domain. Therefore, we next asked whether TET1 regulates DNA demethylation and alters epigenetic modifications around FXBS.

TET1 mediates active epigenetic modification at FOXA1-dependent enhancers

To determine whether TET1 affects the epigenetic environment at FOXA1-occupied enhancers, we first tested whether TET1 is able to co-occupy FOXA1-bound genomic regions. As human anti-TET1 antibody has not been well-established for ChIP, we transfected HA-tagged TET1 into LNCaP prostate cancer cells, validated by western blot in Supplementary Figure S8 and performed ChIP using ChIP-grade anti-HA antibody. ChIP-qPCR confirmed much stronger HA (TET1) enrichment at FXBS in cells expressing HA-TET1 than cells transfected with HA-control vector (Figure 5A). Next, to examine how TET1 alters DNA methylation around these FOXA1-bound regions, we performed TET1 knockdown using shRNA (Figure 5B). Western blots of different exposure times were included to show that TET1 was detected much more strongly at 150 kD, while also giving a very weak band above 250 kD, both of which were depleted upon shRNA knockdown (Supplementary Figure S5D). As TET1 is a DNA demethylase that catalyzes 5mC–5hmC, we next sought to determine the level of 5hmC and 5mC in TET1-knockdown cells. Dot blot experiment confirmed significant reduction of total 5hmC abundance in shTET1 cells (Supplementary Figure S9A). Further, hMe-Seal-seq revealed a remarkable decrease of total 5hmC-enriched regions following TET1 knockdown (Figure 5C). By contrast, 5mC as measured by MeDIP-seq was increased nearly 33% (Figure 5D). Average intensity view of all peaks showed that hMe-Seal signals were significantly decreased, while MeDIP signals increased upon TET1-knockdown (Figure 5E and Supplementary Figure S9B). Focused analysis of these epigenetic modifications around FXBS confirmed an overall decrease of 5hmC and increase of 5mC following TET1 depletion, suggesting that TET1 is critical for the maintenance of the demethylated state of these enhancers (Figure 5F and G). As DNA methy-

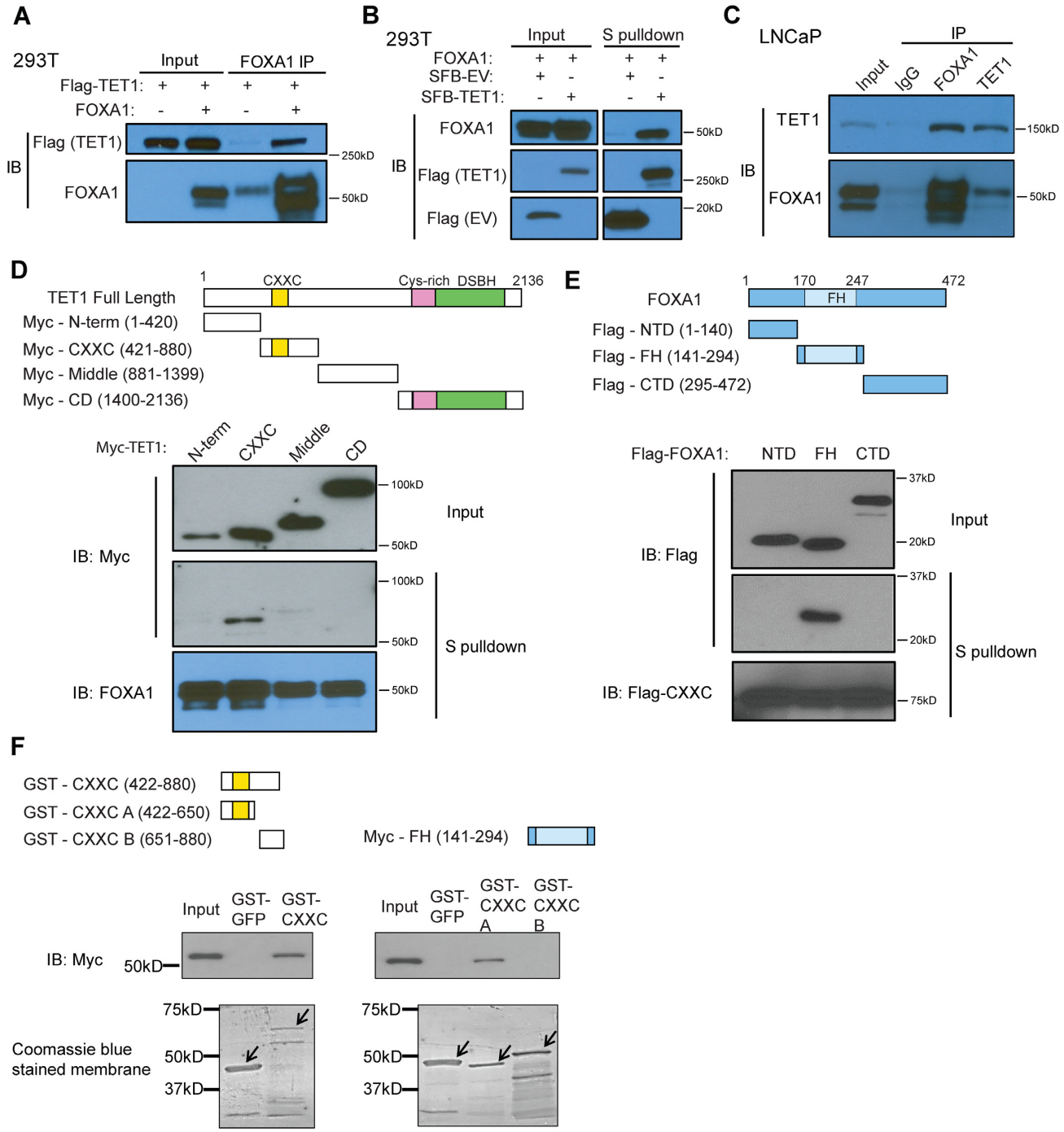

Figure 4. FOXA1 and TET1 proteins physically interact. (**A**) Immunoprecipitation of ectopic FOXA1 pulled down TET1 protein. The 293T cells were transfected with Flag-TET1, either alone or together with FOXA1, for 48 h and then subjected to immunoprecipitation using an FOXA1 antibody. Whole cell (Input) and IP-enriched lysates were then analyzed by western blotting using anti-Flag (TET1) and anti-FOXA1 antibodies. (**B**) Ectopic TET1 immunoprecipitation pulled down FOXA1 protein. The 293T cells were co-transfected with FOXA1 and SFB-tagged empty vector (EV) or TET1 for 48 h before immunoprecipitation using S beads, which will pull down SFB-EV or SFB-TET1. The input and IP-enriched cell lysates were then subjected to western blotting using anti-FOXA1 and anti-Flag (for SFB-EV or SFB-TET1) antibodies. (**C**) Endogenous FOXA1 and TET1 proteins interact in LNCaP cells. LNCaP cells were subjected to immunoprecipitation using anti-FOXA1, anti-TET1 and IgG control, followed by western blotting of FOXA1 and TET1 proteins. (**D**) TET1 CXXC domain interacts with the FOXA1 protein. 293T cells were co-transfected with SFB-FOXA1 along with various Myc-tagged TET1 domain constructs. The expression of TET1 domains in whole cell lysate (input) was confirmed by western blotting using anti-Myc. Cell lysates were then subjected to S pull down (of FOXA1) and subsequently western blot analysis using anti-FOXA1 and anti-Myc antibodies. (**E**) FOXA1 FH (Forkhead-containing) domain interacts with TET1 CXXC domain. 293T cells were co-transfected with SFB-CXXC along with various Flag-tagged FOXA1 domain constructs and subjected to S pull down (of TET1-CXXC) followed by western blotting using an anti-Flag antibody. (**F**) *Invitro* interaction assay was conducted using purified proteins of TET1 CXXC domain and FOXA1 Forkhead domain. CXXC domain was tagged with GST and further subdivided into fragments A and B (the 'C-X-X-C' motif was located in residues 590–609 in fragment A), and FH domain was tagged with Myc. Arrows point to expression of proteins according to their expected size.

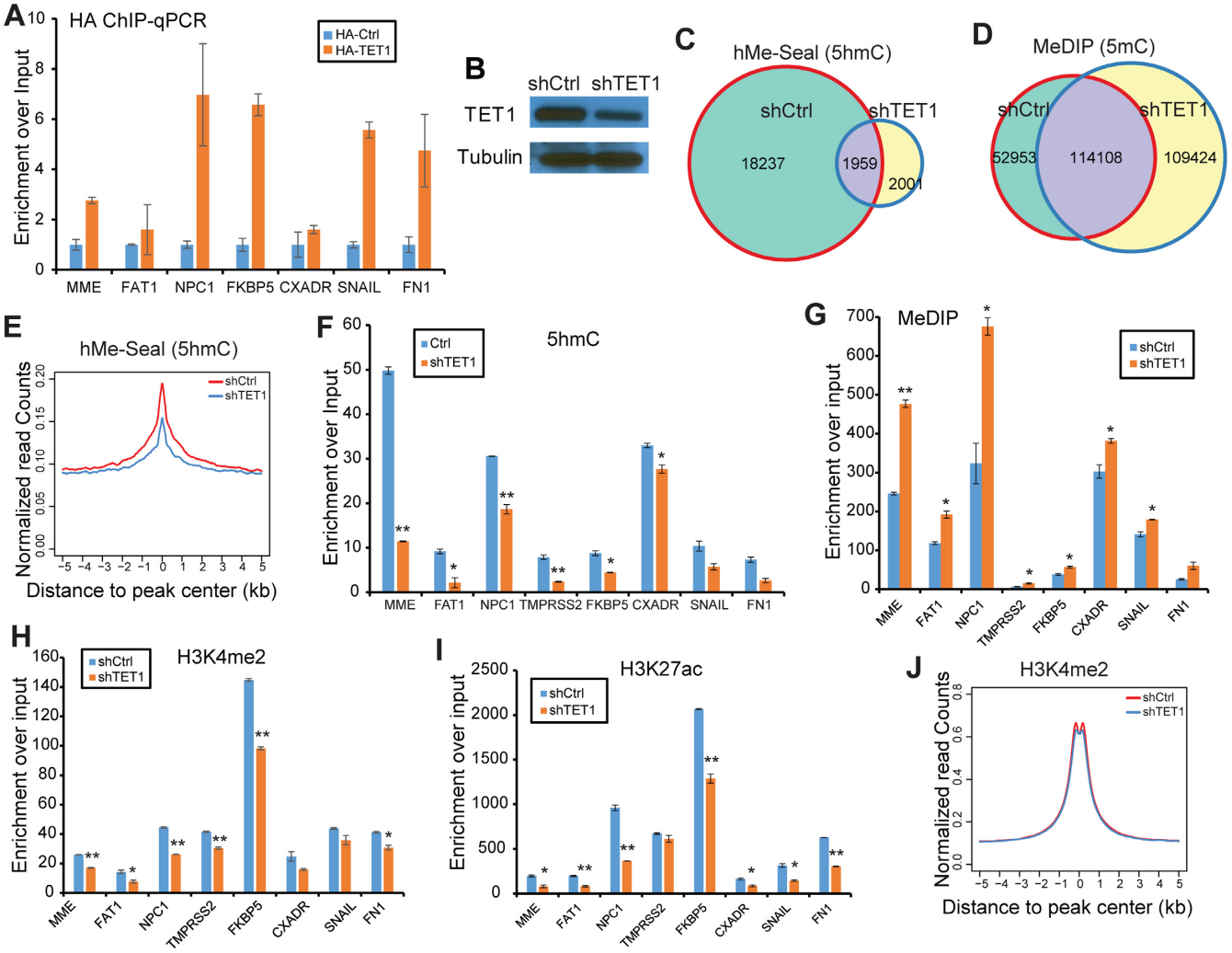

Figure 5. TET1 mediates active epigenetic modification at FOXA1-bound enhancers. (**A**) TET1 co-occupies FXBS. LNCaP cells were transfected with HA-tagged empty vector or TET1 constructs and were subsequently used for ChIP with anti-HA antibody. HA ChIP-qPCR was performed using primers flanking a number of FXBS. Data shown are mean ± SEM of technical replicates from one representative experiment out of three. (**B**) Western blots confirming TET1 knockdown. LNCaP cells were infected with either scramble or shTET1 lentivirus followed by puromycin selection for 4 days before western blot analysis. Tubulin is used as a loading control. (**C** and **D**) Venn Diagrams showing alterations in global genomic regions enriched for 5hmC (C) and 5mC (D) following TET1 knockdown. LNCaP cells with control or shTET1 were subjected to hMe-Seal-seq and MeDIP-seq for genome-wide location analysis of 5hmC and 5mC, respectively, which were subsequently compared between control and TET1-depleted cells. (**E**) Average intensity plot of normalized hMe-Seal-seq reads around (±5 kb) FXBS. (**F**–**I**) TET1 knockdown led to altered epigenetic signatures at FXBS. LNCaP cells with control or TET1 knockdown were subjected to hMe-Seal (F) and MeDIP (G) and ChIP using anti-H4K4me2 (H) and anti-H3K27ac (I) antibodies, followed by qPCR analysis with site-specific primers. Data shown are mean ± SEM of technical replicates from one representative experiment out of two. $*P < 0.05$ and $**P < 0.01$. (**J**) Average intensity plots of normalized H3K4me2-seq reads around (±5 kb) FXBS.

lation has been shown to inhibit enhancer activation (7), we next asked whether TET1 knockdown prohibits enhancer activation at FXBS. ChIP-qPCR showed that indeed H3K4me2 and H3K27ac were both significantly reduced following TET1 depletion (Figure 5H and I). ChIP-seq further confirmed a global decrease of H3K4me2 level in TET1-knockdown (Figure 5J). Taken together, our data support that TET1 expression contributes to the activation of FOXA1-target enhancers through mediating active DNA demethylation.

TET1 expression is required for FOXA1 recruitment to target enhancers

Since it has been reported that DNA methylation and removal of H3K4me2 could impair FOXA1 binding (5,7), the changes in DNA methylation and histone modification events observed following TET1 depletion were suggestive of disrupted FOXA1 recruitment to these regions. To test this, we performed FOXA1 ChIP-seq in control and TET1-knockdown LNCaP cells to determine whether TET1 depletion is able to regulate FOXA1 chromatin targeting. A global assessment of the total binding events before and after TET1 knockdown demonstrated that a significant proportion of FOXA1 binding events were lost upon

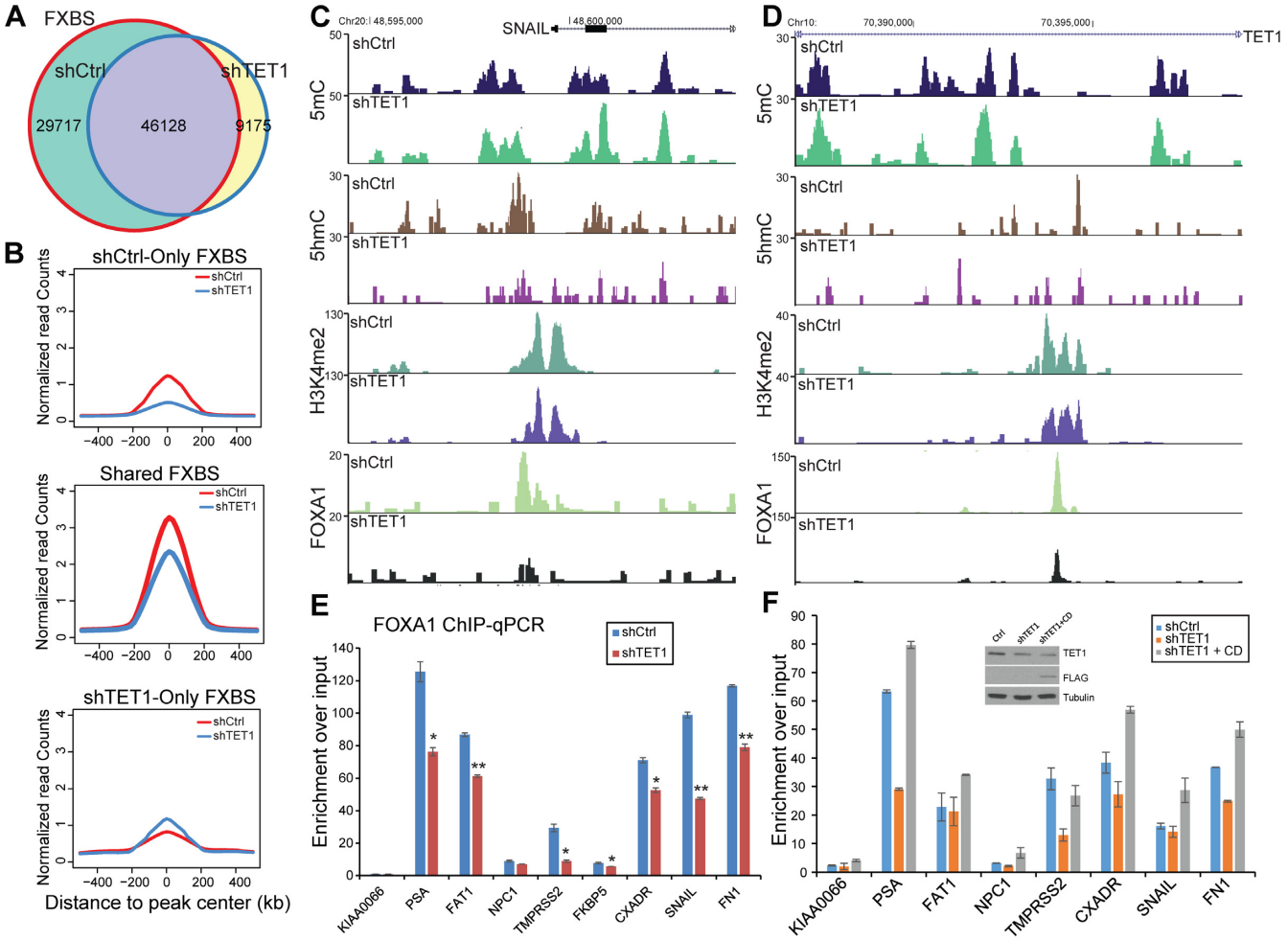

Figure 6. TET1 is required for FOXA1 recruitment to lineage-specific enhancers. (**A**) Venn diagram showing overlap of FXBS in control and FOXA1-knockdown LNCaP cells. (**B**) Average FOXA1 ChIP-seq read intensity around (±500 bp) shCtrl-only, shared and shTET1-only FXBS identified from overlap Venn diagram in (A). (**C** and **D**) Genome browser views of epigenetic modifications at the regulatory regions of FOXA1-target genes SNAIL (C) and TET1 itself (D). MeDIP-seq (5mC), hMe-Seal-seq (5hmC), H3K4me2 and FOXA1 ChIP-seq were performed in control and TET1-knockdown LNCaP cells. For each mark, the shCtrl and shTET1 tracks are shown on the same scale (Y-axis) for visual comparison of enrichment. (**E**) TET1 depletion attenuates FOXA1 recruitment to target enhancers. ChIP-qPCR was performed in control and shTET1 LNCaP cells using anti-FOXA1 antibody. Data shown are mean ± SEM of technical replicates from one representative out of triplicate experiments. $*P < 0.05$ and $**P < 0.01$. (**F**) Impaired FOXA1 recruitment in TET1-depleted cells is restored by TET1 CD overexpression. LNCaP cells were subjected to control or TET1 knockdown with or without concomitant TET1 CD overexpression. TET1 knockdown and CD domain (Flag-CD) overexpression were confirmed by western blot analysis (inset). Cells were subsequently used for ChIP with an anti-FOXA1 antibody followed by qPCR analysis. Data shown are mean ± SEM of technical replicates from one representative of duplicate experiments.

TET1 depletion (Figure 6A). The total number of FXBS was decreased from 76 000 to 55 000. In addition, the average intensity of FOXA1 binding events appeared to be much weaker even for the sites that were not fully abolished (i.e. shared sites) following TET1 knockdown (Figure 6B). Genome browser view of several FOXA1-dependent enhancers further illustrated significant loss of FOXA1 occupancy in TET1-depleted cells (Figure 6C and D; Supplementary Figure S10A and B). Meanwhile, DNA methylation at these enhancers was increased as indicated by enhanced 5mC but reduced 5hmC signals, while active enhancer mark H3K4me2 was decreased, being concordant with the genome-wide switch to repressive chromatin state. Moreover, ChIP-qPCR confirmed that TET1 knockdown significantly decreased FOXA1 occupancy at multiple target enhancers (Figure 6E).

As TET1 interacts with the FOXA1 protein through its CXXC domain but is known to carry out enzymatic activities through its CD domain, we next attempted to understand mechanistically whether CD-mediated DNA demethylation is sufficient to facilitate FOXA1 recruitment to target enhancers. A recent study has reported an interesting and important observation that the CD domain of TET proteins induces massive global DNA demethylation, whereas the function of full-length TET1 is much restricted to unmethylated CpG islands (24). We thus predict that CD domain may be able to restore FOXA1 recruitment in TET1-knockdown cells. To test this, we overexpressed the CD domain in LNCaP cells with TET1 knockdown. ChIP-

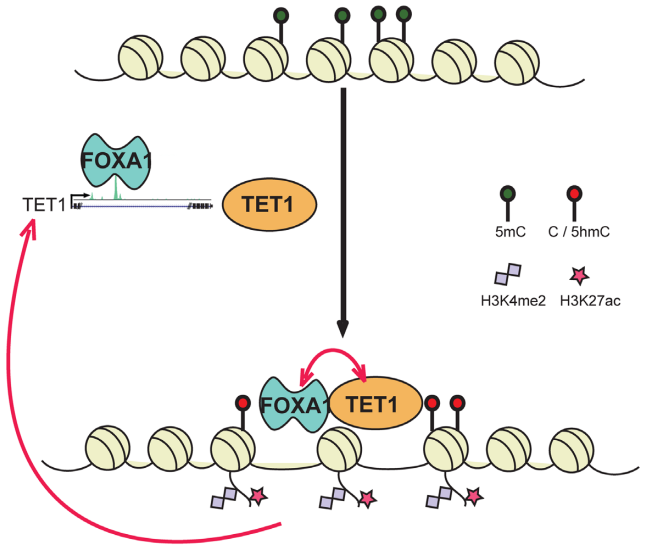

Figure 7. Schematic model depicting feed-forward regulation between FOXA1 and TET1 in lineage-specific enhancer activation. FOXA1 protein occupies at an intragenic enhancer of the TET1 gene to induce TET1 expression. Through direct interaction with FOXA1 protein, TET1 modulates DNA demethylation and subsequently H3K4 methylation and H3K27 acetylation at FOXA1-target enhancers, which in turn facilitates FOXA1 recruitment. Thus, FOXA1 and TET1 form a positive feedback loop in lineage-specific enhancer activation. FOXA1 is not only capable of recognizing but also modifying epigenetic signatures at lineage-specific enhancers.

qPCR confirmed that FOXA1 binding at target enhancers was decreased by TET1 knockdown, which, importantly, can be fully rescued by concomitant CD domain overexpression (Figure 6F). Taken together, our data support that TET1 facilitates FOXA1 recruitment to target enhancers through active demethylation.

DISCUSSION

FOXA1 is a critical regulator of hormone-mediated gene expression in prostate and breast cancers. Much efforts have been devoted to understand the molecular basis for FOXA1's activity as a pioneer factor and studies in the past two decades have helped to paint a clearer picture of how FOXA1 activity is dependent on a number of epigenetic signatures that exhibit lineage specificity (5). Although FOXA1 has been shown to impose some effects on the epigenetic signatures around target enhancers (5), the molecular mechanisms by which FOXA1 remodels heterochromatin remain largely unknown. In the present study, we show that FOXA1 is able to directly regulate the transcription of *TET1* gene. Further, FOXA1 physically interacts with the TET1 protein, leading to DNA demethylation and H3K4me2/H3K27ac modifications at FOXA1-target enhancers. These changes in the epigenetic environment on the other hand enhance FOXA1 recruitment. Therefore, our data support a model wherein FOXA1 is not only able to recognize and bind enhancer regions, but contributes to *de novo* gain of H3K4 methylation and enhancer activation. The latter is mediated by, at least in part, a feed-forward loop between FOXA1 and TET1 where FOXA1 induces TET1 expression and binding at lineage-specific enhancers, which in turn facilitates and stabilizes FOXA1 recruitment through catalyzing DNA demethylation (Figure 7). Accompanying changes in DNA methylation are also reductions in H3K4me2 and H3K27ac upon FOXA1 depletion. Whether these are secondary to DNA demethylation or FOXA1/TET1 may regulate histone methyltransferases such as MLL are areas for future investigation.

TET1 has been implicated in the regulation of enhancer activation and lineage differentiation through DNA demethylation (13,14), the underlying mechanism of which, however, remains elusive. In this report, using prostate cancer cells as a model system, we demonstrated that TET1 contributes to FOXA1 recruitment to prostate-specific enhancers by modulating local epigenetic switch. In future studies, it will be interesting to investigate and compare how TET1 regulates epigenetic marks and FOXA1 recruitment in breast cancer, since FOXA1 has been shown to bind distinct, lineage-specific enhancers in prostate and breast cells (5). In addition, this study will pave the way to further investigation of how TET1, through modulation of FOXA1-dependent enhancer activation, regulates hormone-dependent gene expression and prostate and breast cancer progression.

The CXXC domain of TET proteins has been shown critical for specific chromatin targeting, while the CD domain modulates its enzymatic activity (23). Further, a recent study has reported that the full-length TET1 protein preferably binds to unmethylated CpG islands through its CXXC domain (24). Being consistent with these reports, we found that FOXA1 interacts with TET1 protein through its CXXC domain. Such interaction may be critical for targeting TET1 to prostate-specific enhancers denoted by FOXA1, which may be interesting lines for further investigation utilizing various TET1 deletion constructs and ChIP-seq experiments. Moreover, TET1 might similarly interact with other lineage-defining transcription factors and get recruited to distinct, lineage-specific enhancers in different cell types. By contrast, overexpression of the TET1 CD domain alone has been shown to induce massive global DNA demethylation (24). Indeed, in our study we found overexpression of CD domain is able to rescue the effects of TET1 knockdown on FOXA1 recruitment to target enhancers. Therefore, through interaction with other transcription factors, TET1 achieves its specificity to bind selected enhancers, where it carries out its role in the maintenance of hypomethylated landscape and regulation of lineage differentiation.

In conclusion, FOXA1 is a multipotent pioneer transcription factor, which is impressively capable of chromatin remodeling through not only histone displacement but also DNA demethylation by employing the DNA hydroxylase TET1. Collectively, through regulation of TET1 expression and function, FOXA1 is able to control the epigenetic signatures present at its cis-regulatory elements through a feed-forward loop, ultimately giving rise to chromatin relaxation and enhancer activation.

SUPPLEMENTARY DATA

Supplementary Data are available at NAR Online.

ACKNOWLEDGEMENTS

We would like to thank Dr Debabrata Chakravarti for providing the shTET1 construct.
Author contributions: Y.A.Y, K.F., J.K., S.L., C.S., B.S. and B.Z. performed the experiments. J.C.Z performed all bioinformatics analysis. J.Y. conceived and supervised the project. J.Y. and Y.A.Y. designed the experiments. C.H. supervised the MeDIP-seq and hMe-Seal-seq experiments. J.Y., Y.A.Y. and J.C.Z generated the figures and wrote the manuscript. All authors discussed the results, commented on the manuscript and declare no conflicts of interest.

FUNDING

U.S. Department of Defense [W81XWH-13-1-0319 to J.Y., in part]; American Cancer Society Research Scholar Award [RSG-12-085-01 to J.Y.]; National Institutes of Health [R01HG006827 to C.H.]; Howard Hughes Medical Institute (to C.H.); NIH/NCI training grant [T32 CA09560 to Y.A.Y., in part]; NIH Training Program in Oncogenesis and Developmental Biology [T32 CA080621 to J.K., in part]. Funding for open access charge: National Institutes of Health [R01-CA172384 to J.Y.].
Conflict of interest statement. None declared.

REFERENCES

1. Bernardo,G.M. and Keri,R.A. (2012) FOXA1: a transcription factor with parallel functions in development and cancer. *Biosci. Rep.*, **32**, 113–130.
2. Gao,N., Ishii,K., Mirosevich,J., Kuwajima,S., Oppenheimer,S.R., Roberts,R.L., Jiang,M., Yu,X., Shappell,S.B., Caprioli,R.M. *et al.* (2005) Forkhead box A1 regulates prostate ductal morphogenesis and promotes epithelial cell maturation. *Development*, **132**, 3431–3443.
3. Bernardo,G.M., Lozada,K.L., Miedler,J.D., Harburg,G., Hewitt,S.C., Mosley,J.D., Godwin,A.K., Korach,K.S., Visvader,J.E., Kaestner,K.H. *et al.* (2010) FOXA1 is an essential determinant of ERalpha expression and mammary ductal morphogenesis. *Development*, **137**, 2045–2054.
4. Jozwik,K.M. and Carroll,J.S. (2012) Pioneer factors in hormone-dependent cancers. *Nat. Rev. Cancer*, **12**, 381–385.
5. Lupien,M., Eeckhoute,J., Meyer,C.A., Wang,Q., Zhang,Y., Li,W., Carroll,J.S., Liu,X.S. and Brown,M. (2008) FoxA1 translates epigenetic signatures into enhancer-driven lineage-specific transcription. *Cell*, **132**, 958–970.
6. Wang,J., Zhuang,J., Iyer,S., Lin,X., Whitfield,T.W., Greven,M.C., Pierce,B.G., Dong,X., Kundaje,A., Cheng,Y. *et al.* (2012) Sequence features and chromatin structure around the genomic regions bound by 119 human transcription factors. *Genome Res.*, **22**, 1798–1812.
7. Serandour,A.A., Avner,S., Percevault,F., Demay,F., Bizot,M., Lucchetti-Miganeh,C., Barloy-Hubler,F., Brown,M., Lupien,M., Metivier,R. *et al.* (2011) Epigenetic switch involved in activation of pioneer factor FOXA1-dependent enhancers. *Genome Res.*, **21**, 555–565.
8. Gifford,C.A. and Meissner,A. (2012) Epigenetic obstacles encountered by transcription factors: reprogramming against all odds. *Curr. Opin. Genet. Dev.*, **22**, 409–415.
9. Tahiliani,M., Koh,K.P., Shen,Y., Pastor,W.A., Bandukwala,H., Brudno,Y., Agarwal,S., Iyer,L.M., Liu,D.R., Aravind,L. *et al.* (2009) Conversion of 5-methylcytosine to 5-hydroxymethylcytosine in mammalian DNA by MLL partner TET1. *Science*, **324**, 930–935.
10. Ito,S., Shen,L., Dai,Q., Wu,S.C., Collins,L.B., Swenberg,J.A., He,C. and Zhang,Y. (2011) Tet proteins can convert 5-methylcytosine to 5-formylcytosine and 5-carboxylcytosine. *Science*, **333**, 1300–1303.
11. Maurano,M.T., Wang,H., John,S., Shafer,A., Canfield,T., Lee,K. and Stamatoyannopoulos,J.A. (2015) Role of DNA methylation in modulating transcription factor occupancy. *Cell Rep.*, **12**, 1184–1195.
12. Feldmann,A., Ivanek,R., Murr,R., Gaidatzis,D., Burger,L. and Schubeler,D. (2013) Transcription factor occupancy can mediate active turnover of DNA methylation at regulatory regions. *PLoS Genet.*, **9**, e1003994.
13. Serandour,A.A., Avner,S., Oger,F., Bizot,M., Percevault,F., Lucchetti-Miganeh,C., Palierne,G., Gheeraert,C., Barloy-Hubler,F., Peron,C.L. *et al.* (2012) Dynamic hydroxymethylation of deoxyribonucleic acid marks differentiation-associated enhancers. *Nucleic Acids Res.*, **40**, 8255–8265.
14. Hon,G.C., Song,C.X., Du,T., Jin,F., Selvaraj,S., Lee,A.Y., Yen,C.A., Ye,Z., Mao,S.Q., Wang,B.A. *et al.* (2014) 5mC oxidation by Tet2 modulates enhancer activity and timing of transcriptome reprogramming during differentiation. *Mol. Cell*, **56**, 286–297.
15. Robinson,J.L., Holmes,K.A. and Carroll,J.S. (2013) FOXA1 mutations in hormone-dependent cancers. *Front. Oncol.*, **3**, 20.
16. Yu,J., Yu,J., Mani,R.S., Cao,Q., Brenner,C.J., Cao,X., Wang,X., Wu,L., Li,J., Hu,M. *et al.* (2010) An integrated network of androgen receptor, polycomb, and TMPRSS2-ERG gene fusions in prostate cancer progression. *Cancer Cell*, **17**, 443–454.
17. Yu,J., Cao,Q., Yu,J., Wu,L., Dallol,A., Li,J., Chen,G., Grasso,C., Cao,X., Lonigro,R.J. *et al.* (2010) The neuronal repellent SLIT2 is a target for repression by EZH2 in prostate cancer. *Oncogene*, **29**, 5370–5380.
18. Song,C.X., Clark,T.A., Lu,X.Y., Kislyuk,A., Dai,Q., Turner,S.W., He,C. and Korlach,J. (2012) Sensitive and specific single-molecule sequencing of 5-hydroxymethylcytosine. *Nat. Methods*, **9**, 75–77.
19. Wang,D., Garcia-Bassets,I., Benner,C., Li,W., Su,X., Zhou,Y., Qiu,J., Liu,W., Kaikkonen,M.U., Ohgi,K.A. *et al.* (2011) Reprogramming transcription by distinct classes of enhancers functionally defined by eRNA. *Nature*, **474**, 390–394.
20. Jin,H.J., Zhao,J.C., Wu,L., Kim,J. and Yu,J. (2014) Cooperativity and equilibrium with FOXA1 define the androgen receptor transcriptional program. *Nat. Commun.*, **5**, 3972.
21. Song,C.X., Szulwach,K.E., Fu,Y., Dai,Q., Yi,C., Li,X., Li,Y., Chen,C.H., Zhang,W., Jian,X. *et al.* (2011) Selective chemical labeling reveals the genome-wide distribution of 5-hydroxymethylcytosine. *Nat. Biotechnol.*, **29**, 68–72.
22. Fong,K.W., Leung,J.W., Li,Y., Wang,W., Feng,L., Ma,W., Liu,D., Songyang,Z. and Chen,J. (2013) MTR120/KIAA1383, a novel microtubule-associated protein, promotes microtubule stability and ensures cytokinesis. *J. Cell Sci.*, **126**, 825–837.
23. Xu,Y., Xu,C., Kato,A., Tempel,W., Abreu,J.G., Bian,C., Hu,Y., Hu,D., Zhao,B., Cerovina,T. *et al.* (2012) Tet3 CXXC domain and dioxygenase activity cooperatively regulate key genes for Xenopus eye and neural development. *Cell*, **151**, 1200–1213.
24. Jin,C., Lu,Y., Jelinek,J., Liang,S., Estecio,M.R., Barton,M.C. and Issa,J.P. (2014) TET1 is a maintenance DNA demethylase that prevents methylation spreading in differentiated cells. *Nucleic Acids Res.*, **42**, 6956–6971.